The Kinetic Mechanism of Cation-Catalyzed Phosphatidylglycerol Transbilayer Migration Implies Close Contact between Vesicles as an Intermediate State†

Barry R. Lentz,*,‡ Nancy A. Whitt,‡ Dennis R. Alford,‡,§ Stephen W. Burgess,‡ Julie C. Yates,‡ and Shlomo Nir‖

Department of Biochemistry, University of North Carolina, Chapel Hill, North Carolina 27599-7260, and The Hebrew University Faculty of Agriculture, Rehovot 76100, Israel

Received September 7, 1988; Revised Manuscript Received February 9, 1989

ABSTRACT: We have investigated variations in the rate of Mn^{2+}-catalyzed phosphatidylglycerol transbilayer migration [Lentz, Madden, & Alford (1982) *Biochemistry 21*, 6799] with changes in phospholipid and cation concentration over more than a 100-fold range of both parameters. The slope of a double logarithmic plot of the rate of transbilayer lipid migration versus lipid concentration was 1.7, suggesting that lipid redistribution was dependent on vesicle aggregation or collision. A model involving transitory dimerization of vesicles was able to account for the concentration dependence of the transbilayer redistribution rate. The observed variation in rate with the logarithm of Mn^{2+} concentration was complex: linear above 0.4 μM (corresponding to roughly 2.5 Mn^{2+} per vesicle) but involving a steeper dependence on Mn^{2+} below 0.04 μM (roughly four vesicles per Mn^{2+}). The rate of transbilayer redistribution increased substantially between 37 and 56 °C, yielding a nonlinear Arrhenius plot. There was no evidence of either fusion or lipid exchange between vesicles at the low concentrations of Mn^{2+} needed for transbilayer redistribution. The data are consistent with a model suggesting transitory "micro-domains" of a dehydrated, interbilayer complex as involved in the transition state and are inconsistent with a model involving an inverted micelle-type structure for the transition state.

Small, unilamellar vesicles (SUV)[1] prepared from mixtures of phosphatidylglycerol (PG) and phosphatidylcholine (PC) by sonication (but in the absence of exposure to metal sonication probes) demonstrate an asymmetric transbilayer distribution of PG and PC, such that a disproportionate amount of PG is found in the outer leaflet of the vesicle bilayer (Lentz et al., 1980). We have shown previously (Lentz et al., 1982) that catalytic levels of Mn^{2+} or Cd^{2+} induce the transbilayer redistribution of PG in these SUV. Remarkably, this catalytic ability was highly specific for Cd^{2+} and Mn^{2+}; seven other divalent or trivalent metal ions were ineffective. In addition, transbilayer lipid migration took place in this system without disruption of the bilayer permeability barrier. The detailed molecular mechanism by which this cation-induced "flip-flop" occurs is an enigma.

Transbilayer lipid migration normally occurs very slowly in model lipid bilayers (Shaw et al., 1977) but can take place much more rapidly in biological membranes (Bloj & Zilversmit, 1976; van Deenen, 1981). In both native membranes (Zachowski et al., 1986) and model membranes (Greenhut & Roseman, 1985), proteins catalyze this process. The role of cations in this catalysis is not known.

Both with the hope of obtaining insights into the mechanism of transbilayer lipid migration in biomembranes and with the goal of better defining the highly specific ion–lipid interactions required for this phenomenon, we present data that establish a kinetic model for the cation-induced flip-flop of PG in PG/PC SUV. These data establish a ternary vesicle–ion–vesicle complex as the intermediate state in the flip-flop process. In addition, lipid exchange, vesicle aggregation, and vesicle contents mixing data are presented that argue aganst an intervesicular inverted micellar structure serving as an intermediate state in the flip-flop process. We suggest that ion-induced loose aggregation of PG/PC vesicles destabilizes bilayer structure, perhaps through disruption of the membrane hydration layer, sufficiently to allow transmembrane lipid redistribution but not enough to induce leakage, intervesicle lipid exchange, or vesicle fusion.

Materials and Methods

1,2-Dipentadecanoyl-3-*sn*-phosphatidylglycerol ($DC_{15}PG$),[1] 1,2-dimyristoyl-3-*sn*-phosphatidylcholine (DMPC),[1] 1-palmitoyl-2-oleoyl-3-*sn*-phosphatidylcholine (POPC),[1] and 1,2-dioleoyl-3-*sn*-phosphatidylglycerol (DOPG)[1] were purchased from Avanti Polar Lipids (Birmingham, AL) and shown to be greater than 98% pure by thin-layer chromatography (Lentz et al., 1980). DMPC and POPC were stocked in argon-bubbled chloroform while $DC_{15}PG$ and DOPG were stored as their sodium salts in 1/1 chloroform/methanol. Solvents were of low-residue, HPLC grade. Concentrations of the stock solutions were established by inorganic phosphate determination (Chen et al., 1956). Calcium ion contamination of the PG (PC) was shown to be less than 2 mol % (1 mol %) (Lentz et al., 1982).

All chemicals were of reagent grade or better. Ultrapure salts were obtained from Alpha Ventron (Danvers, MA). Water for buffers was distilled from basic potassium permanganate and then redistilled from a Pyrex flask, saturated with argon, and stored in borosilicate glass bottles at 4 °C until

† Supported by USPHS Grant GM32707 to B.R.L.

* To whom correspondence should be addressed.

‡ University of North Carolina.

§ Present address: Department of Pharmaceutical Chemistry, School of Pharmacy, University of California, San Francisco, CA 94143.

‖ The Hebrew University Faculty of Agriculture.

[1] Abbreviations: PG, phosphatidylglycerol; PC, phosphatidylcholine; DOPG, 1,2-dioleoyl-3-*sn*-phosphatidylglycerol; POPC, 1-palmitoyl-2-oleoyl-3-*sn*-phosphatidylcholine; $DC_{15}PG$, 1,2-dipentadecanoyl-3-*sn*-phosphatidylglycerol; DMPC, 1,2-dimyristoyl-3-*sn*-phosphatidylcholine; DPHpPC, 1-palmitoyl-2-[[2-[4-(6-phenyl-*trans*-1,3,5-hexatrienyl)-phenyl]ethyl]carbonyl]-3-*sn*-phosphatidylcholine; DPHpPG, 1-palmitoyl-2-[[2-[4-(6-phenyl-*trans*-1,3,5-hexatrienyl)phenyl]ethyl]carbonyl]-3-*sn*-phosphatidylglycerol; SUV, small, unilamellar vesicles; Na_2EDTA, disodium ethylenediaminetetraacetate.

0006-2960/89/0428-4575$01.50/0

used. Sodium cacodylate for the PG assay buffer was purchased from Polysciences, Inc., and recrystallized before use (Lentz et al., 1982b).

Preparation of Small, Unilamellar Vesicles. Appropriate mixtures of lipids were prepared in chloroform/methanol and dried under a stream of argon onto the wall of an annealed glass ampule and then further dried under high vacuum for 6–12 h. Appropriate buffer was added to suspend the samples at a lipid concentration of 2–20 mM, and they were sonicated with a Heat Systems W350 sonicator (Heat Systems-Ultrasonics, Inc., Plainview, NY) equipped with a Heat Systems Cup Horn (Barrow & Lentz, 1980). Vesicles were fractionated by ultracentrifugation (Barenholz et al., 1977). All manipulations were performed at temperatures such that the lipids remained in their liquid-crystalline (fluid) phase at all times (Lentz et al., 1982a).

Assay for Phosphatidylglycerol Transbilayer Distribution. As documented previously (Lentz et al., 1980, 1982b), we assayed for PG by oxidation with periodate followed by detection of the resulting formaldehyde through the development of a colored adduct with chromotropic acid. This was quantitated through its absorbance at 579 nm. In order to use this assay to detect transbilayer PG distribution, we performed the periodate oxidation on intact as well as sodium dodecyl sulfate solubilized vesicles at temperatures at which all lipids were in the fluid phase. The mild oxidation conditions left the vesicle permeability barrier intact for about 22 min, sufficient time to oxidize all the outer-leaflet PG (Lentz et al., 1980). From the time course of oxidation, then, we obtained the ratio of exposed, outer-leaflet PG to total PG ($PG_{out}/PG_{tot} = R$).

Kinetics of Transbilayer PG Redistribution. PG redistribution was initiated by adding Mn^{2+} at appropriate concentrations to $DC_{15}PG/DMPC$ (1/1 molar ratio) vesicles at time zero. At various times thereafter, a portion of the vesicle sample was added to 0.3 mM Na_2EDTA to halt the Mn^{2+}-induced redistribution process. These quenched samples were then assayed to obtain the exposed to total PG ratio (R). The time course for each redistribution process was analyzed according to the equations:

$$PG_{out} + PC_{in} \underset{k_2}{\overset{k_1}{\rightleftharpoons}} PG_{in} + PC_{out} \quad (1)$$

$$d[PG_{out}]/dt = -k_1[PG_{out}] + k_2[PG_{in}] \quad (2)$$

which has the solution

$$R - R_{eq} = (R_0 - R_{eq}) \exp(-Kt) \quad (3)$$

where R_0 and R_{eq} are the exposed to total ratios at zero time and very long time (i.e., equilibrium), respectively, with $K = k_1 + k_2$ and $R_{eq} = k_2/K$.

Vesicle Lipid Mixing, Contents Mixing, and Aggregation. Intervesicular exchange of membrane lipids was monitored by using the concentration sensitivity of the fluorescence lifetime of phospholipids containing the fluorescent moiety, 1,6-diphenyl-1,3,5-hexatriene, DPHpPG,[1] and DPHpPC[1] (Parente & Lentz, 1985). In this procedure, vesicles containing a high concentration of DPH-labeled lipid (4 mol % for DPHpPC and 2 mol % for DPHpPG) were mixed with vesicles free of probe, and an increase of fluorescence excited-state lifetime was taken to indicate exchange of lipid between the two vesicle populations (Parente & Lentz, 1986a). Fluorescence lifetimes were measured on an SLM 48000 phase fluorometer (SLM-Aminco Instruments, Urbana, IL) operating at a modulation frequency of 30 MHz and using diphenylhexatriene in heptane as an isochronal standard (τ = 6.75 ns, 0.2 μM; Barrow & Lentz, 1983). Excitation was with a 200-W Hg–Xe lamp (PTI, Inc., Princeton, NJ) using the 366-nmHg spectral line. Other details of these measurements are given elsewhere (Parente & Lentz, 1985). The mixing of vesicle contents was determined by using the water-soluble fluorophore/quencher pair: disodium 8-aminonaphthalene-1,3,6-trisulfonate (ANTS)/*N,N'-p*-xylylenebis(pyridinium bromide) (DPX) (Ellens et al., 1984). The details of this method are given elsewhere (Ellens et al., 1984; Parente & Lentz, 1986); briefly, when vesicles containing the naphthalene fluorophore fuse with vesicles containing the pyridinium quencher, a drop in fluorescence is observed. The extent of this drop, relative to the fluorescence from vesicles containing coencapsulated fluorophore and quencher, gives the extent of fusion.

Vesicle aggregation was monitored in the SLM 48000 fluorometer as an increase in 90° light scattering at 366 nm following addition of Mn^{2+} to a vesicle suspension.

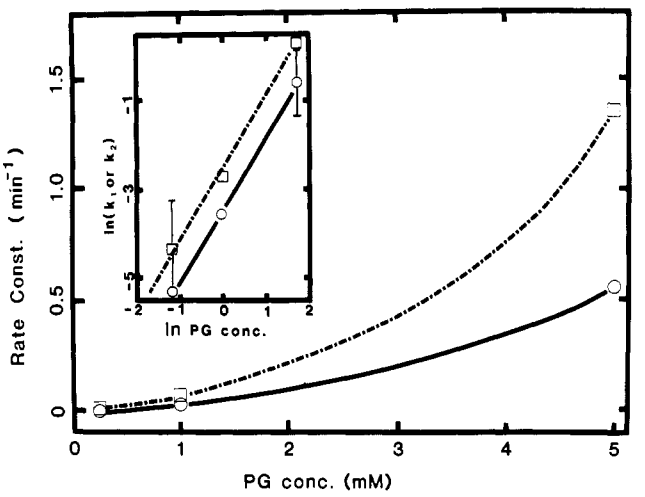

FIGURE 1: Lipid concentration dependence of the rates (k_1, solid line; k_2, dashed line) of phospholipid transbilayer redistribution in 1/1 $DC_{15}PG/DMPC$ SUV at a Mn^{2+} concentration of 40 nM. The insert shows the data plotted in a log–log fashion, yielding straight lines with slopes of 1.7. Error bars in the log–log plot represent the standard error ($\pm\sigma$) derived from the uncertainties in the slopes of logarithmic plots of the kinetic data (eq 3); except as indicated, these were smaller than the symbols representing each data point.

Results and Discussion

Lipid and Ion Concentration Dependence of Kinetic Constants. The kinetics of $DC_{15}PG$ transbilayer migration in $DC_{15}PG/DMPC$ (1/1) vesicles were determined at 37 °C at a Mn^{2+} concentration of 40 nM and three lipid concentrations. At this temperature, these vesicles are in the fluid, liquid-crystalline phase (Lentz et al., 1982a). An example of the determination of lipid redistribution kinetic constants from measurements of outer-to-inner leaflet PG (R) is given in Figure 3 of Lentz et al. (1982b). Such kinetic experiments were extremely difficult to perform, leading us to plan carefully so as to obtain the maximum of mechanistic information from the minimum number of experiments. The forward and reverse rate constants determined in this way are plotted in Figure 1 of this paper as a function of PG concentration. The inset to Figure 1 shows a double logarithmic plot of the data, demonstrating that the rate of PG flip-flop varies according to the 1.7 ± 0.3 power of phospholipid concentration. This means that the Mn^{2+}-induced transbilayer redistribution process is second order in lipid concentration, implying a contact-dependent process. In the Appendix, we present a detailed kinetic analysis in terms of a dynamic dimerization model. This shows that a dimerization (or aggregation, in general) process with kinetics comparable to the kinetics of

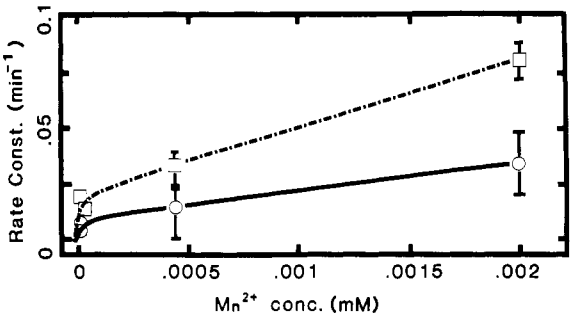

FIGURE 2: Ion concentration dependence of the rates (k_1, solid line; k_2, dashed line) of phospholipid transbilayer redistribution in 1/1 $DC_{15}PG$/DMPC SUV at a $DC_{15}PG$ concentration of 0.24 mM. Error bars were obtained as described for Figure 1. For the sake of clarity, error bars were omitted for the data at low Mn^{2+} concentration. At very low Mn^{2+} concentration, the data demonstrated a steeper dependence but then became clearly linear at higer ion concentrations.

lipid redistribution can account for the slope of slightly less than 2 in the logarithmically transformed data in Figure 1.

We have also investigated the dependence of flip-flop kinetics on the concentration of Mn^{2+} used to induce this process. The results (shown in Figure 2) demonstrate a linear relationship at 0.4 μM and above but a steeper relationship below 0.04 μM. This behavior suggests Mn^{2+} binding to PG is the major factor affecting flip-flop kinetics, which appear to depend on vesicle–vesicle interactions. It has been shown (Nir, 1984) that the amount of a trace element bound to a membrane in a closed system is linearly related to the total amount of that element in the system. Apparently, a steeper dependence of the rate of flip-flop on the Mn^{2+} concentration occurs in the range where there are between 0.25 and 2.5 cations per vesicle (i.e., between 0.04 and 0.4 μM Mn^{2+}), suggesting that roughly one cation per vesicle is necessary for the flip-flop process.

Vesicle Aggregation and Fusion Induced by Mn^{2+}. The results summarized in Figures 1 and 2 suggest that two (or possibly more) vesicles joined by Mn^{2+} ions are crucial to the lipid transbilayer redistribution process. If this were the case, it might be possible to detect aggregation of the vesicles upon addition of Mn^{2+}. Under the conditions of the experiments summarized in Figures 1 and 2 ([Mn^{2+}] = 20 nM to 2 μM; [PG] = 0.1–5.0 mM), no aggregation of $DC_{15}PG$/DMPC vesicles could be detected either by eye or by 90° light scattering. However, as documented in Figure 3, higher concentrations of Mn^{2+} did elicit small but measurable changes in light scattering that were reversible, at least up to 20 mM Mn^{2+}, by addition of Na^2EDTA. It is clear that stable aggregation is not required for the lipid redistribution process, but it is still completely conceivable that low concentrations of Mn^{2+} might form weak vesicle–vesicle contacts sufficient to induce flip-flop.

Much larger and irreversible light scattering changes were found for pure $DC_{15}PG$ vesicles treated with greater than 5 mM Mn^{2+} (Figure 3), an observation consistent with published reports of Ca^{2+}-induced PG vesicle fusion (Papahadjopoulos et al., 1976; Rosenberg et al., 1983), binding of millimolar Mn^{2+} to PG vesicles (Pushkin & Martin, 1979), and induction by Mn^{2+} of a dehydrated, aggregated state in PG bilayers (Boggs & Rangaraj, 1983). These results indicate that high concentrations of Mn^{2+} could cause fusion of pure PG or even PG-rich SUV. However, as we have previously reported (Lentz et al., 1982b), there is no evidence that the extremely low levels of Mn^{2+} needed to induce flip-flop cause vesicle fusion. This has been confirmed here by direct fluorescence assay of vesicle contents mixing and leakage (Ellens et al., 1984; see Materials and Methods). Thus, no contents mixing or leakage were observed in 1/1 DOPG/POPC SUV even in a medium containing 2 μM Mn^{2+} at 20 °C (data not shown), conditions shown previously to induce rapid flip-flop (Lentz et al., 1982b).

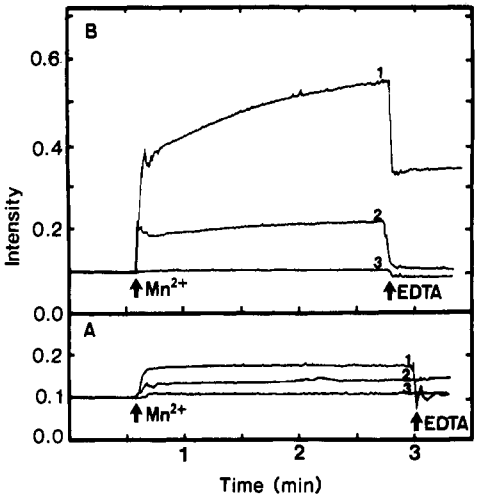

FIGURE 3: 90° light scattering data for (A) $DC_{15}PG$–DMPC (50:50) and (B) $DC_{15}PG$ SUV at 45 °C. (A) Vesicles (SUV; 0.2 mM lipid) were incubated with (1) 50 mM Mn^{2+}, (2) 20 mM Mn^{2+}, and (3) 5 mM Mn^{2+}. (B) Vesicles (SUV; 0.2 mM lipid) were incubated with (1) 15 mM Mn^{2+}, (2) 5 mM Mn^{2+}, and (3) 0.05 mM Mn^{2+}. Both vesicle populations were incubated with Mn^{2+} for 2.5 min before Na_2EDTA was added.

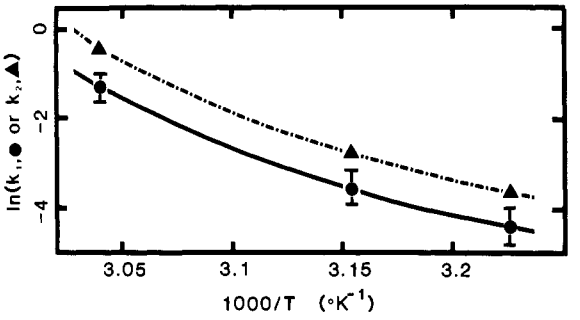

FIGURE 4: Arrhenius plots of the temperature dependence of the rates (k_1, solid line; k_2, dashed line) of phospholipid transbilayer redistribution in 1/1 $DC_{15}PG$/DMPC SUV at a Mn^{2+} concentration of 40 nM and a PG concentration of 1 mM. The error bars were obtained as described in Figure 1 and were the same for k_2 as for k_1. The nonlinear nature of these plots makes it impossible to obtain the activation energy from the slopes (see text).

Temperature Dependence of Kinetic Constants. In order to obtain greater insight into the mechanism of transbilayer redistribution, kinetic measurements were made at two additional temperatures. The data from these experiments are summarized in an Arrhenius form in Figure 4, which indicates a nonlinear increase in the logarithm of the redistribution kinetic constants with temperature. Transition-state rate theory predicts a linear Arrhenius plot when the ΔH^* term dominates the temperature dependence of ln k and when ΔH^* and ΔS^* are temperature-independent. Nonlinear behavior of an Arrhenius plot makes a simple activation energy analysis impossible, as the point slope of such a plot can greatly overestimate the activation energy (Nir et al., 1980). However, from the large increase in rate with temperature, it is clear that the barrier to flip-flop, and therefore the activation free energy, is considerably reduced at higher temperatures. This could reflect a decrease in ΔH^* or an increase in ΔS^* with temperature. It is reasonable to presume that exposing membrane interior to water would be increasingly favored at higher temperatures, given the larger fluctuations in lipid

packing density to be expected. Our results are consistent with the intermediate state in the redistribution process involving such a disordering fluctuation in bilayer structure. This would presumably become less entropically unfavorable relative to the average bilayer thermodynamic state at high temperature.

Models for Molecular Mechanism of Flip-Flop. It is not difficult to envision a molecular mechanism and accompanying destabilized state that might account for our data. An immediately apparent but poorly detailed description is that vesicle–vesicle collisions could transiently perturb bilayer structure so as to encourage flip-flop. Despite the apparent simplicity of this mechanism, the involvement of Mn^{2+} in the process would require very improbable three-body collisions. A more likely and certainly more detailed mechanism that comes to mind is the inverted micelle-type structure shown in Figure 5A. Such structures have been proposed to be involved in the bilayer destabilization responsible for membrane fusion (Siegel, 1987). It is also possible that Mn^{2+}-induced bilayer juxtaposition alters water structure in the interbilayer space, thereby altering and destabilizing the bilayer structure. One possible scheme for this is illustrated in Figure 5B, in which we show lipid order increased in a very small, local region of Mn^{2+}-induced interbilayer contact. This is consistent with the known formation of a dehydrated, ordered phase upon incubating phosphatidylglycerol with millimolar Mn^{2+} (Boggs & Rangaraj, 1983). Our cartoon illustrates that the formation of such a local, interbilayer "micro-domain" would necessitate disrupted lipid packing in the interface between this domain and the bulk lipid bilayer. This is similar to the disrupted lipid bilayer that we have previously proposed to surround transmembrane proteins (Lentz et al., 1985). Both the inverted micellar state and the dehydrated, interbilayer complex are envisioned here as existing only as infrequent fluctuations as opposed to thermodynamically stable features of membrane structure. Both are capable of disrupting packing in such a way as to expose the hydrophobic portion of the bilayer to water. In this thermodynamically unfavorable state, the movement of lipid molecules across the bilayer would be less unfavorable a process than in the unperturbed bilayer—i.e., the free energy of Mn^{2+}-induced dimerization lowers the free energy barrier of the flip-flop process.

Intervesicle Lipid Exchange. The two molecular mechanisms suggested in Figure 5 differ in their prediction with regard to intervesicular exchange of lipid. The inverted micelle mechanism (Figure 5A) specifically predicts that lipids should freely exchange between vesicles during aggregation, while the mechanism in Figure 5B does not imply lipid exchange. In order to distinguish between these two types of mechanisms, we performed experiments designed to detect the exchange of DPH-labeled PG and PC between vesicles in response to the addition of Mn^{2+}. In these experiments, vesicles containing a high concentration of labeled lipid (4 mol %) were incubated with unlabeled vesicles, and the fluorescence excited-state lifetime was recorded as a function of time. Under these conditions, the observed lifetime was only 3.7 ns, reflecting the high concentration of probe in the one lipid population (Parente & Lentz, 1986a). Lipid mixing between vesicles should be indicated by an increase in lifetime.

Results are summarized in Figure 6 and Table I. For $DC_{15}PG$/DMPC/DPHpPC (50/46/4) vesicles incubated with $DC_{15}PG$/DMPC vesicles at 45 °C, exchange of DPHpPC between labeled and unlabeled vesicles was observed even in the absence of Mn^{2+} (Figure 6). However, the rate of this exchange did not change upon addition of Mn^{2+}. A similar experiment with DOPG/POPC vesicles performed at 23 °C showed a similar result (Figure 6). That both temperature and degree of unsaturation contributed to enhanced rates of lipid exchange is demonstrated by data obtained at 40 °C with DOPC/DOPG and DMPC/$DC_{15}PG$ vesicles (Table I). Finally, an experiment was performed with DOPG/POPC/DPHpPG (46/50/4) and DOPG/POPC (1/1) vesicles at 23 °C (Figure 6). Again, no Mn^{2+}-induced lipid exchange was observed. Under the conditions of these experiments, the observed exponential time constant for decay of transbilayer asymmetry was 8–9 min. Therefore, if lipid exchange were associated with the transbilayer redistribution process, it should have been observed during the time courses examined in Figure 6. We conclude that neither DPHpPC nor DPHpPG are exchanged between vesicles in response to Mn^{2+} and, therefore, that the inverted micelle model in Figure 5A is untenable as a mechanism to explain Mn^{2+}-induced flip-flop.

Conclusions

Mn^{2+}-induced lipid transbilayer redistribution is facilitated by vesicle–vesicle interaction, apparently mediated by low concentrations of Mn^{2+}. The times required for PG redistribution varied from 30 s to 2 h, depending on the range of Mn^{2+} and lipid concentrations employed. The kinetic transition state for this process apparently involves the transient disruption of bilayer structure in the aggregated state. The data are consistent with a model suggesting local domains of a dehydrated, interbilayer complex as involved in the transition state but are inconsistent with a model involving an inverted micelle-type structure for the transition state.

Appendix

Dynamic Aggregation Model. We propose that the Mn^{2+}-induced transbilayer redistribution of PG occurs mainly through a kinetic transition state involving intimate contact between two (or more) vesicles. Aggregation is presumably mediated though Mn^{2+}. The change in PG asymmetry can be described in terms of the rates of transbilayer movement in the aggregated transition state:

$$dR/dt = d[PG_{out}]/dt = (-f_1^*[PG_{out}]^* + f_2^*[PG_{in}]^*)/PG_{tot} \quad (A1)$$

where R is the ratio of exposed to total PG as defined under Materials and Methods and

$$[PG_{out}]^* = \gamma[PG_{out}][V_2(t)]$$
$$[PG_{in}]^* = \gamma[PG_{in}][V_2(t)] \quad (A2)$$

are the concentrations of outer- and inner-leaflet PG in the aggregated state. Since the fraction of aggregated vesicles is very small, we consider only the concentration of vesicle dimers, $[V_2(t)]$. γ is a proportionality constant for adjusting units, and $[PG_{out}]$ and $[PG_{in}]$ are the *total* outer- and inner-leaflet PG concentrations. It must be stressed that, in the treatment considered here (Nir et al., 1980), $[V_2(t)]$ is a dynamic quantity, and the observed rate of flip-flop will reflect not only the rate of transbilayer lipid redistribution but also the rate of the Mn^{2+}-dependent, reversible aggregation step.

With rearrangement, eq A1 becomes

$$dR(t)/dt = \{-(f_1 + f_2)R(t) + f_2\}[V_2(t)] \quad (A3)$$

where $f_i = \gamma f_i^*$. In the case where $V_2(t)$ rapidly reaches a steady-state value, $V_2(\infty)$, we can substitute $k_i = f_i V_2(\infty)$ and obtain an expression equivalent to eq 2 under Materials and Methods.

Equation A3 was solved numerically by using a Taylor series expansion with $[V_2(t)]$ constrained to satisfy mass conservation.

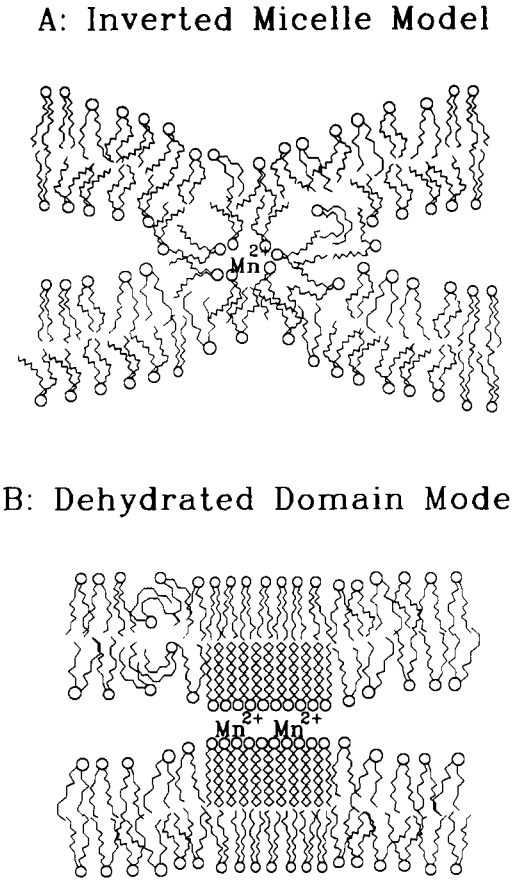

FIGURE 5: Hypothetical molecular arrangements in the transition state for Mn^{2+}-induced phospholipid transbilayer redistribution in PG/PC SUV: (A) inverted micelle-type structure; (B) disrupted bilayer due to closely apposed dehydrated domain.

Table I: Summary of Rates of Lipid Mixing of SUV in the Presence of 0.44 μM Mn^{2+}

lipid system	temp (°C)	% lipid mixing/ min[a]
POPC	23	0.035
POPC/DOPG (50:50)	23	0.110
DMPC[b]	45	1.590
DMPC/DC_{15}PG (50:50)	45	0.780
POPC/DOPG (50:50)	40	1.710
DMPC/DC_{15}PG (50:50)	40	0.440
POPC/DOPG (50:50)[c]	23	0.460

[a] Expressed as the percentage of total lifetime change expected when lipids are completely exchanged. [b] No Mn^{2+} added to the vesicle suspension. [c] Using DPHpPG as a probe of lipid exchange.

The details of this calculation are essentially the same as the treatment of aggregation kinetics given by Bentz and Nir (1981). The numerical simulations were run in Basic on an Apple II microcomputer. The dimerization equilibrium constants ($\alpha = C_{11}/D_{11}$), corresponding to aggregation (C_{11}) and disaggregation (D_{11}) rate constants of 100–500 M^{-1} s^{-1} and 0.01 s^{-1}, respectively, were in the range of 1×10^4–5×10^4 M^{-1}. For the range of lipid concentrations in our experiments (200 μM to 5 mM), this range of dimerization constants results in dimer to total vesicle ratios of 0.0008–0.002, consistent with our light scattering results. The time required to reach equilibrium was about 1 min. In addition, the PG redistribution kinetic constants (K in eq 3) calculated from these simulations varied exponentially with lipid concentration, with powers of 1.85–2.0 ($\alpha = 1 \times 10^4$ M^{-1}) or 1.75–1.90 ($\alpha = 5 \times 10^4$ M^{-1}). We conclude that this dynamic aggregation model can account for the results we have obtained for the kinetics of transbilayer lipid redistribution in DC_{15}PG/DMPC SUV.

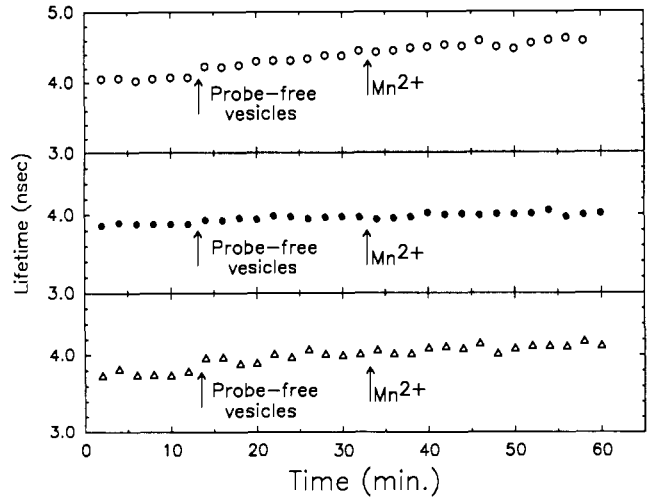

FIGURE 6: Test for Mn^{2+}-induced DPHpPC exchange between 1/1 DC_{15}PG/DMPC vesicles at 45 °C (upper curve) and between 1/1 DOPG/POPC vesicles at 23 °C (middle curve) and of DPHpPG between 1/1 DOPG/POPC vesicles at 23 °C (lower curve). Probe-containing vesicles were examined at a concentration of 23 μM, and at the arrow, probe-free vesicles were added to a total PG concentration of 0.25 mM. Mn^{2+} was added at the second arrow to a concentration of 2 μM. If complete lipid mixing were to occur in response to Mn^{2+}, the final lifetimes would be 6.0 ns for DPHpPC and 5.8 ns for DPHpPG.

References

Barenholz, Y., Gibbs, D., Litman, B. J., Goll, J., Thompson, T. E., & Carlson, F. D. (1977) *Biochemistry 16*, 2806–2810.

Barrow, D. A., & Lentz, B. R. (1980) *Biochim. Biophys. Acta 597*, 92–99.

Barrow, D. A., & Lentz, B. R. (1983) *J. Biochem. Biophys. Methods 7*, 217–234.

Bentz, J., & Nir, S. (1981) *J. Chem. Soc., Faraday Trans. 177*, 1249–1275.

Bloj, B., & Zilversmit, D. B. (1976) *Biochemistry 15*, 1277–1283.

Boggs, J. M., & Rangaraj, G. (1983) *Biochemistry 22*, 5425–5435.

Chen, P. S., Jr., Toribara, T. Y., & Warner, H. (1956) *Anal. Chem. 23*, 1756–1758.

Ellens, H., Bentz, J., & Szoka, F. C. (1984) *Biochemistry 23*, 1532–1538.

Greenhut, S. F., & Roseman, M. A. (1985) *Biochemistry 24*, 1252–1260.

Lentz, B. R., Alford, D. R., & Dombrose, F. A. (1980) *Biochemistry 19*, 2555–2559.

Lentz, B. R., Alford, D. R., Hoechli, M., & Dombrose, F. A. (1982a) *Biochemistry 21*, 4212–4219.

Lentz, B. R., Madden, S., & Alford, D. R. (1982b) *Biochemistry 21*, 6799–6807.

Lentz, B. R., Clubb, K. W., Alford, D. R., Höchli, M., & Meissner, G. (1985) *Biochemistry 24*, 433–442.

Nir, S. (1984) *J. Colloid Interface Sci. 102*, 313–321.

Nir, S., Bentz, J., & Portis, A. R., Jr. (1980) *Adv. Chem. Ser. No. 188*, 75–106.

Papahadjopoulos, D., Vail, W. J., Pangborn, W. A., & Poste, G. (1976) *Biochim. Biophys. Acta 448*, 265–283.

Parente, R. A., & Lentz, B. R. (1985) *Biochemistry 24*, 6178–6185.

Parente, R. A., & Lentz, B. R. (1986a) *Biochemistry 25*, 1021–1026.

Parente, R. A., & Lentz, B. R. (1986b) *Biochemistry 25*,

6678-6688.
Pushkin, J. S., & Martin, T. (1979) *Biochim. Biophys. Acta 552*, 53-65.
Rosenberg, J., Düzgünes, N., & Kayalar, C. (1983) *Biochim. Biophys. Acta 735*, 173-180.
Shaw, J. M., Hutton, W. C., Lentz, B. R., & Thompson, T. E. (1977) *Biochemistry 16*, 4156-4163.
Siegel, D. P. (1987) in *Cell Fusion* (Sowers, A. E., Ed.) pp 181-207, Plenum Publishing Corp., New York.
van Deenen, L. L. M. (1981) *FEBS Lett. 123*, 3-15.
Zachowski, A., Favre, E., Cribier, S., Hervé, P., & Devaux, P. F. (1986) *Biochemistry 25*, 2585-2690.

Analysis of Protein-Mediated 3-*O*-Methylglucose Transport in Rat Erythrocytes: Rejection of the Alternating Conformation Carrier Model for Sugar Transport†

Amy L. Helgerson and Anthony Carruthers*

Department of Biochemistry, University of Massachusetts Medical Center, 55 Lake Avenue North, Worcester, Massachusetts 01605

Received August 10, 1988; Revised Manuscript Received January 4, 1989

ABSTRACT: 3-*O*-Methylglucose (3OMG) transport in rat erythrocytes (RBCs) is mediated by a low-capacity, facilitated diffusion-type process. This study examines whether the characteristics of sugar transport in rat RBCs are consistent with the predictions of two diametric, theoretical mechanisms for sugar transport. The *one-site carrier* describes a transport mechanism in which sugar influx and efflux substrate binding sites are mutually exclusive. The *two-site carrier* describes a transport mechanism in which sugar influx and efflux substrate binding sites can exist simultaneously but may interact in a cooperative fashion when occupied by substrate. Michaelis and velocity parameters for saturable 3OMG transport in rat erythrocytes at 24 °C were obtained from initial rate measurements of 3OMG transport. The results are incompatible with the predictions of the one-site carrier but are consistent with the predictions of a symmetric two-site carrier, displaying negligible cooperativity between substrate binding sites. This allows reduction of the two-site carrier transport equations to a form containing fewer constants than the one-site carrier equations without limiting their predictive success. While the available evidence does not prove that rat erythrocyte sugar transport is mediated by a two-site mechanism, we conclude that adoption of the formally more complex one-site model for sugar transport in rat erythrocytes in unnecessary and unwarranted. Counterflow experiments have also been performed in which the time course of radiolabeled 3OMG uptake is measured in cells containing saturating levels of 3OMG. The results of these experiments are consistent with the hypothesis [Naftalin et al. (1985) *Biochim. Biophys. Acta 820*, 235-249] that exchange of sugar between intracellular compartments (cell water and hemoglobin) can be rate limiting for transport under certain conditions.

Passive, saturable sugar transport in eukaryotic cells is mediated by an integral membrane protein(s) of 42-60-kDa molecular mass (Mueckler et al., 1985; Birnbaum et al., 1986; Allard & Lienhard, 1985). While the functional and structural properties of sugar transport systems may display subtle species and tissue differences (e.g., in stereoselectivity for sugars, heterogeneity of transporter glycosylation, sensitivity to inhibitors, susceptibility to physiological regulation, etc.), the similarities between the systems studied to date [with the notable exception of hepatocyte transporter (Birnbaum et al., 1986) and the insulin-sensitive adipocyte carrier (James et al., 1988)] suggest both a common evolutionary origin and a common catalytic mechanism (Mueckler et al., 1985; Birnbaum et al., 1986).

The catalytic mechanism of sugar transport is the subject of some controversy. A variety of theoretical transport models have been proposed to account for the facilitated diffusion of D-glucose (DG)[1] across human red cell membranes. These include the classical asymmetric one-site (mobile or alternating conformer) carrier (Widdas, 1952; Regen & Tarpley, 1974), the asymmetric two-site (linear or simultaneous) carrier (Baker & Widdas, 1973), the tetramer model (Lieb & Stein, 1971), the allosteric pore model (Holman, 1980), the bi-antiparallel asymmetric one-site system (Ginsburg, 1978), the symmetric two-site carrier model rate limited by intracellular water and sugar complexation (Naftalin & Holman, 1977; Naftalin et al., 1985), and the two-site allosteric carrier model (Helgerson & Carruthers, 1987). Each of these models fails to account for some of the experimental properties of red cell sugar transport [for reviews of these and additional models, see Naftalin and Holman (1977) and Stein (1986)]. This has led a number of workers to propose that the apparent complexity of human erythrocyte hexose transfer results from technical problems associated with transport determinations rather than

† This work was supported by National Institutes of Health Grant RO1 AM36081.
* Author to whom correspondence should be addressed.

[1] Abbreviations: CCB, cytochalasin B; CCD, cytochalasin D; CCE, cytochalasin E; 3OMG, 3-*O*-methyl-α-D-glucopyranoside; DG, D-glucose; Hb, hemoglobin; P_{sat}, permeability coefficient for protein-mediated transport; K_L, rate constant for transmembrane sugar leakage; RBC, red blood cell.

0006-2960/89/0428-4580$01.50/0